Ab initio Calculations on Excited Molecular Ions of Ethylene and Acetylene*

Ernest R. Davidson and Yan A. Wang

Chemistry Department, Indiana University,
Bloomington, IN 47405, USA.

Abstract

Ab initio calculations of the energy and wave functions for neutral molecules and excited molecular ions are used to interpret the EMS and PES spectra of acetylene and ethylene. The five satellite regions of acetylene are assigned to intensity borrowed from $2\sigma_g$, $3\sigma_g$ and $2\sigma_u$ primary hole states by ion states with configurations $(\pi_u)^{-2} (2\delta_g)^1$, $(\pi_u)^{-2} (3\sigma_g)^{-1} (\pi_g)^2$, and $(\pi_u)^{-1} (3\sigma_g)^{-1} (\pi_g)^1$. The Dyson orbitals for the satellite regions of acetylene and ethylene are shown to differ from the Dyson orbitals of the primary holes. The importance of choosing basis sets appropriate to the excited states of the ion is illustrated.

1. Introduction

We have developed programs for computing energies and wave functions for highly excited states using configuration interaction with extended basis sets. These programs have been used in recent collaborative studies with Brion and Bawagan for acetylene, C_2H_2 (Moghaddam *et al.* 1995; Duffy *et al.* 1992*b*) and ethylene, C_2H_4 (Desjardins *et al.* 1994; Hollebone *et al.* 1995; Desjardins *et al.* 1995). Over the past few years we have studied the EMS spectrum of a large number of molecules in collaboration with the experimental work of Brion. These include CH_4 (Clark *et al.* 1990), NH_3 (Bawagan *et al.* 1988*b*), H_2O (Bawagan *et al.* 1987; Duffy *et al.* 1992*a*), HF (Hollebone *et al.* 1993*c*; Davidson *et al.* 1990), PH_3 (Clark *et al.* 1989*a*), H_2S (French *et al.* 1988*b*), HCl (Hollebone *et al.* 1993*a*), H_2CO (Bawagan *et al.* 1988*a*; Hollebone *et al.* 1993*b*; Rossi and Davidson 1992), $H(CH_3)CO$ (Hollebone *et al.* 1993*b*; Rossi and Davidson 1992), $(CH_3)_2CO$ (Hollebone *et al.* 1993*b*; Rossi and Davidson 1992), $(CH_3)NH_2$ (Maxwell *et al.* 1992), SiH_4 (Clark *et al.* 1989*b*) and CO (French *et al.* 1988*a*). Ongoing work that is not yet published includes He, H_2, O_2 and NO. In the past, we have also considered the many-body effects on the PES and XAFS of a few molecules such as C_2H_4 (Martin and Davidson 1977*a*; Murray and Davidson 1992), halogen atoms and diatomics (Martin and Davidson 1977*b*; Rehr *et al.* 1978), Na (Martin *et al.* 1978) and Ne (Martin *et al.* 1979).

Our present programs cannot handle continuum wave functions. Hence, we cannot actually calculate the cross sections for EMS or PES. Instead, we rely

on an approximate cancellation of transition matrix elements to give the relative
PES intensities, and assume the plane wave impulse approximation to obtain
estimates of the EMS spectrum. If electron correlation between the ion wave
function and the outgoing electron can be neglected, the ion wave function
approximately factors into the antisymmetrised product of $|\Psi^+\rangle$ and a continuum
orbital χ. Assuming χ is orthogonal to all the orbitals used in constructing the
wave function $|\Psi\rangle$ for the neutral molecule, the usual electric dipole transition
moment can be calculated in two steps as

$$\phi = \langle \Psi | \Psi^+ \rangle_{N-1} \,, \tag{1}$$

which defines the Dyson orbital ϕ as the integral over the $N-1$ electrons of the
cation followed by

$$\boldsymbol{M} = \langle \chi | \boldsymbol{r} | \phi \rangle \,. \tag{2}$$

It has been found empirically that most neutral molecules can be described to
good accuracy by a single Slater determinant using Hartree–Fock orbitals. While
the coefficient of this determinant decreases exponentially with the number of
electrons, it is typically an order of magnitude larger than the next coefficient
in an expansion in Slater determinants. Some of the states of the ion can
be described to a fair approximation as having a hole in one of the canonical
Hartree–Fock orbitals of the neutral. Canonical orbitals are ones that diagonalise
the Fock operator and, by Koopmans' theorem, provide the best description of
the ion using just the occupied orbitals of the neutral molecule. These states are
often referred to as 'primary hole states' in PES. Apart from normalisation, their
Dyson orbitals are nearly the occupied orbitals of the neutral molecule. The
square of the normalisation constant for the Dyson orbital is commonly called
the 'pole strength'

$$S^2 = \langle \phi | \phi \rangle \,. \tag{3}$$

Other states of the ion are most simply described as having two holes and an
excited electron $(2h-1p)$ relative to the neutral. From the point of view of ordinary
molecular spectroscopy of the cation, these states are just valence-Rydberg single
excitations from a primary hole state. In the formula for the Dyson orbital, the
integral for the neutral molecule Hartree–Fock configuration with a $2h-1p$ ion
configuration is zero. Relaxation and electron correlation often cause the ion
state to include primary hole configurations with small coefficients. When only
one primary hole state contributes appreciably, the Dyson orbital, apart from
normalisation, will resemble the Dyson orbital of the primary hole state. When
that is true, the ratio

$$\frac{|\boldsymbol{M}_p|^2}{|\boldsymbol{M}_q|^2} = \frac{|\langle \chi_p | \boldsymbol{r} | \phi_p \rangle|^2}{|\langle \chi_q | \boldsymbol{r} | \phi_q \rangle|^2} \tag{4}$$

can be simplified by assuming that ϕ_p and ϕ_q differ only in normalisation and
that χ_p and χ_q give the same transition probability. In this case we have

$$\frac{|M_p|^2}{|M_q|^2} = \frac{S_p^2}{S_q^2}.$$

(5)

This model is opposite to the sudden approximation model used for Auger spectra (Åberg 1967; Manne and Åberg 1970; Stöhr *et al.* 1983; Thomas 1984) in that it assumes the molecule is fully relaxed into an exact molecular eigenstate as the electron departs. Nevertheless, this model is often called the sudden approximation where the word 'sudden' implies nothing about time scales, but only that the extent of relaxation of the orbitals in going from the exact neutral state to the exact ion state is small enough that equation (5) applies. The energy of the outgoing electron in PES and EMS is monitored and the subsequent decay of the ion is not followed. There are transitions, of course, for which this mechanism is not dominant, so these approximations are not valid. For example, these approximations suggest that the ratio of satellite to primary hole intensities should be nearly independent of wavelength when the appropriate pairing of $2h$–$1p$ and $1h$ states is made. This is not always true in practice, although it is a very good approximation for the majority of states.

The cross section for (e, 2e) ionisation obeys a similar approximation for the total electron count. If the momentum of the incoming and outgoing electrons is analysed, the more detailed result is that the differential cross section for momentum change

$$\boldsymbol{p} = \boldsymbol{p}_1 + \boldsymbol{p}_2 - \boldsymbol{p}_0$$

(6)

is proportional to the square of the Dyson orbital evaluated at that momentum. This assumes the incoming and outgoing electrons are all described by plane waves, and that the momentum change from neutral molecule to ion is entirely due to the momentum of the electron that is lost (McCarthy and Weigold 1976). For a randomly oriented collection of target molecules, the observed cross section is proportional to the spherical average in momentum space of the square of the Dyson orbital and depends only on the magnitude of $\boldsymbol{p}$.

Thus, in both of these models, the PES and EMS spectra give peaks at the energies of the eigenstates of the ion. The differences from the lowest peak should occur at the same positions as the peaks in the optical spectrum of the ion and all of the peaks can be labeled with an electron configuration, just as would be done in optical spectroscopy. Unfortunately, this is not often done in EMS spectroscopy, but rather the primary peaks are labeled as holes in the neutral molecule, and satellites are labeled by their small component of associated primary hole rather than by their dominant configuration.

There are many ways in which calculations could be carried out for these states. For PES, one should really consider the continuum electron and treat both the neutral molecule and ion as an N electron system, as is done in Green function calculations (Cederbaum *et al.* 1986). For Auger spectroscopy, it has been customary to invoke a sudden approximation in which the ion is formed in a mixed state and subsequently relaxes by emission of photons and additional electrons (Åberg 1967; Manne and Åberg 1970; Stöhr *et al.* 1983; Thomas 1984). For EMS, the calculation should really be done as a scattering event with $N+1$ electrons throughout the process.

In the quantum chemical approach followed here, we look for exact excited states of the ion. In the energy range of interest, extending up to about 30 eV above the neutral ground state, there are more than 100 excited states of the ion for the small molecules considered here. Consequently, we begin with a large set of basis functions sufficient for describing the neutral molecule, the ion primary hole states, and the Rydberg excited states of the ion. This is a very extended basis compared to standard basis sets in the literature. Even so, we typically are only able to describe the first few Rydberg orbitals (say $n = 3$ or 4 for atoms with $Z \leq 10$). The EMS spectrum typically only contains data for small p. Roughly speaking, this corresponds to large distances from the nuclei, so the basis set must describe this region accurately. Because the chemical basis sets are linear combinations of Gaussian orbitals rather than Slater orbitals, the long range values are usually underestimated, and the probability of low p is too small. Thus, extended valence basis sets are required for the neutral molecule supplemented with Rydberg basis functions for the excited ion. The ultimate accuracy of the calculation is determined by the basis sets regardless of the method used for the many-electron calculation.

2. Method

To be specific, for the results given here for C_2H_2 and C_2H_4, the basis set consists of $18s$, $13p$, $3d$ and $1f$ Gaussian-type functions on each C centre, contracted to $6s$, $7p$, $3d$, $1f$. On each H centre, there are $10s$, $2p$, $1d$ Gaussians contracted to $5s$, $2p$, $1d$. Also, three p and three d-type Gaussians were placed on the centre of the C_2H_2 molecule and two p and two d sets were placed on the centre of C_2H_4. Since all components of these homogeneous polynomials are kept, a 'd' type Gaussian set contributes an s function as well as the set of five $l = 2$ functions. Similarly, the 'f' set really consists of a complete set of $l = 1$ and $l = 3$ functions. The functions in the centre of the molecule have small exponents appropriate for $n = 3$ states of a cation (i.e. similar to what would be expected for $n = 3$ states of He$^+$). More details are given elsewhere (Moghaddam et $al.$ 1995; Desjardins et $al.$ 1994; Hollebone et $al.$ 1995); Desjardins et $al.$ 1995). Note in particular that this basis spans all the Rydberg orbitals expected for $3s$, $3p$ and $3d$. For example, eight basis functions of δ_g symmetry are included so $3d\delta_g$ can be well-represented for $C_2H_2^+$.

Because of limitations in the program, the calculation of Dyson orbitals requires that the neutral and ion be expanded in Slater determinants built from a common set of molecular orbitals. In many calculations, the molecular orbitals have been chosen as the occupied and virtual canonical Roothaan–Hartree–Fock orbitals of the neutral molecule (as would be used for many-body perturbation theory or Green's functions). In other calculations, an approximation to the neutral natural orbitals has been used (Feller and Davidson 1981). In this paper we have used molecular orbitals determined as the orbitals that diagonalise the average density matrix for excited states of the ion (Desjardins et $al.$ 1994). Because the ions considered here have high symmetry, separate calculations of excited states and average natural orbitals could be done for each molecular wave function irreducible representation. Thus, up to 40 states were involved in each average. The orbitals determined in this way should allow each state to be dominated by a few Slater determinants. Unfortunately in this approach, a new ground state wave function had to be computed from each MO set in order to obtain the Dyson orbitals.

Table 1. Vertical excitation energies to acetylene radical cation states*

	IP (eV)	S^2	PES label			Spectral label
$^2\Pi_u$	11·4	1·64	$(1\pi_u)^{-1}$			X $^2\Pi_u$
$^2\Sigma_g^+$	16·4	0·80	$(3\sigma_g)^{-1}$			$1\pi_u \leftarrow 3\sigma_g$
$^2\Pi_g$	18·5	0·00	$(1\pi_u)^{-2}$	$(1\pi_g)^1$		$1\pi_g \leftarrow 1\pi_u$
$^2\Sigma_u^+$	18·7	0·71	$(2\sigma_u)^{-1}$			$1\pi_u \leftarrow 2\sigma_u$
$^2\Phi_g$	19·4	0·00	$(1\pi_u)^{-2}$	$(1\pi_g)^1$		$1\pi_g \leftarrow 1\pi_u$
$^2\Pi_g$	20·6	0·00	$(1\pi_u)^{-2}$	$(1\pi_g)^1$		$1\pi_g \leftarrow 1\pi_u$
$^2\Sigma_g^+$	23·2	0·52	$(2\sigma_g)^{-1}$			$1\pi_u \leftarrow 2\sigma_g$
$^2\Pi_g$	23·7	0·03	$(1\pi_u)^{-2}$	$(1\pi_g)^1$		$1\pi_g \leftarrow 1\pi_u$
$^2\Sigma_u^+$	23·8	0·01	$(3\sigma_g)^{-1}$	$(1\pi_u)^{-1}$	$(1\pi_g)^1$	$1\pi_g \leftarrow 3\sigma_g$
$^2\Delta_u$	24·0	0·00	$(1\pi_u)^{-2}$	$(3\sigma_u)^1$		$3\sigma_u \leftarrow 1\pi_u$
$^2\Delta_g$	24·4	0·00	$(1\pi_u)^{-2}$	$(5\sigma_g)^1$		$5\sigma_g \leftarrow 1\pi_u$
$^2\Delta_u$	24·8	0·00	$(1\pi_u)^{-1}$	$(3\sigma_g)^{-1}$	$(1\pi_g)^1$	$1\pi_g \leftarrow 3\sigma_g$
$^2\Sigma_g^+$	25·1	0·00	$(1\pi_u)^{-2}$	$(5\sigma_g)^1$		$5\sigma_g \leftarrow 1\pi_u$
$^2\Sigma_u^+$	25·1	0·02	$(1\pi_u)^{-2}$	$(3\sigma_u)^1$		$3\sigma_u \leftarrow 1\pi_u$
$^2\Delta_g$	25·3	0·00	$(1\pi_u)^{-2}$	$(4\sigma_g)^1$		$4\sigma_g \leftarrow 1\pi_u$
$^2\Delta_u$	25·3	0·00	$(1\pi_u)^{-1}$	$(3\sigma_g)^{-1}$	$(1\pi_g)^1$	$1\pi_g \leftarrow 3\sigma_g$
$^2\Pi_u$	25·8	0·00	$(1\pi_u)^{-2}$	$(2\pi_u)^1$		$2\pi_u \leftarrow 1\pi_u$
$^2\Sigma_g^+$	26·0	0·00	$(1\pi_u)^{-2}$	$(4\sigma_g)^1$		$4\sigma_g \leftarrow 1\pi_u$
$^2\Delta_g$	26·3	0·00	$(1\pi_u)^{-2}$	$(1\delta_g)^1$		$1\delta_g \leftarrow 1\pi_u$
$^2\Pi_u$	26·6	0·00	$(1\pi_u)^{-2}$	$(2\pi_u)^1$		$2\pi_u \leftarrow 1\pi_u$
$^2\Delta_g$	26·8	0·00	$(1\pi_u)^{-1}$	$(2\sigma_u)^{-1}$	$(1\pi_g)^1$	$1\pi_g \leftarrow 2\sigma_u$
$^2\Pi_u$	26·9	0·02	$(1\pi_u)^{-2}$	$(2\pi_u)^1$		$2\pi_u \leftarrow 1\pi_u$
$^2\Sigma_g^+$	26·9	0·07	$(1\pi_u)^{-2}$	$(1\delta_g)^1$		$1\delta_g \leftarrow 1\pi_u$
$^2\Delta_g$	27·2	0·00	$(1\pi_u)^{-2}$	$(2\delta_g)^1$		$2\delta_g \leftarrow 1\pi_u$
$^2\Sigma_g^+$	27·3	0·01	$(1\pi_u)^{-2}$	$(1\delta_g)^1$		$1\delta_g \leftarrow 1\pi_u$
$^2\Delta_u$	27·5	0·00	$(1\pi_u)^{-2}$	$(4\sigma_u)^1$		$4\sigma_u \leftarrow 1\pi_u$
$^2\Pi_u$	27·6	0·00	$(1\pi_u)^{-2}$	$(2\pi_u)^1$		$2\pi_u \leftarrow 1\pi_u$
$^2\Sigma_g^+$	28·1	0·11	$(1\pi_u)^{-2}$	$(2\delta_g)^1$		$2\delta_g \leftarrow 1\pi_u$
$^2\Sigma_g^+$	30·3	0·03	$(1\pi_u)^{-2}$	$(3\sigma_g)^{-1}$	$(1\pi_g)^2$	$(1\pi_g)^2 \leftarrow 1\pi_u, 3\sigma_g$
$^2\Sigma_u^+$	30·3	0·03	$(1\pi_u)^{-1}$	$(3\sigma_g)^{-1}$	$(1\pi_g)^1$	$1\pi_g \leftarrow 3\sigma_g$
$^2\Sigma_g^+$	30·8	0·01	$(1\pi_u)^{-1}$	$(3\sigma_g)^{-1}$	$(2\pi_u)^1$	$2\pi_u \leftarrow 3\sigma_g$
$^2\Sigma_g^+$	31·1	0·02	$(3\sigma_g)^{-1}$	$(1\pi_u)^{-2}$	$(1\pi_g)^2$	$(1\pi_g)^2 \leftarrow 1\pi_u, 3\sigma_g$
$^2\Sigma_g^+$	31·7	0·02	$(1\pi_u)^{-1}$	$(3\sigma_g)^{-1}$	$(2\pi_u)^1$	$2\pi_u \leftarrow 3\sigma_g$
$^2\Pi_u$	32·0	0·01	$(1\pi_u)^{-1}$	$(2\sigma_u)^{-1}$	$(3\sigma_u)^1$	$3\sigma_u \leftarrow 2\sigma_u$
$^2\Sigma_u^+$	34·1	0·01	$(1\pi_u)^{-1}$	$(3\sigma_g)^{-1}$	$(2\pi_g)^1$	$2\pi_g \leftarrow 3\sigma_g$

* Only $S = \frac{1}{2}$ states are included; no Σ^- states are included. Beyond 28 eV, only states with large S^2 are included.

Within each irreducible representation, the actual ion wave functions were determined by the multi-reference single and double excitation configuration interaction method. That is, the dominant configurations for each state in the energy range of interest were pooled to define a reference space. This set of configurations was determined iteratively starting from the dominant terms in simple $1h$ and $2h$–$1p$ calculations and including any higher excitations that appeared important in later calculations. Approximate wave functions for all states in the energy range of interest were formed by diagonalisation of the Hamiltonian over this reference set of configurations. All configurations outside of the reference set were then scanned by computing their second order perturbation contribution to each state. Those with contributions beyond some threshold were selected for inclusion in the final configuration interaction wave function. Because the second order energy contribution is zero for any configuration differing

from all reference configurations by more than a double excitation, only single and double excitations get selected. Hence, this method is abbreviated in the chemistry literature as MRSDCI. Its use is well established for the lowest root of each symmetry, and it is occasionally used for the first few states. Its use for a massive search of 100 or more states is unusual. Fortunately, the reference space consisted almost entirely of $1h$ and $2h$–$1p$ configurations with only a few $3h$–$2p$ configurations entering for the highest energy states. Thus, the secondary space selected by the perturbation scan was mostly $3h$–$2p$ and $4h$–$3p$ configurations. These configurations are essential to giving a balanced energy description with the neutral ground state where $2h$–$2p$ configurations (double excitations) describe most of the second-order correlation energy. In fact, in the simplest MBPT expansion, many of the energy contributions from $2h$–$2p$ configurations in the neutral state and $4h$–$3p$ configurations in the $2h$–$1p$ state exactly cancel (although a contribution to the Dyson orbital remains).

Table 2. Vertical excitation energies to ethylene radical cation states[*]

	IP (eV)	S^2	PES label	Spectral label
$^2B_{3u}$	10·5	0·81	$(1b_{3u})^{-1}$	X $^2B_{3u}$
$^2B_{3g}$	12·9	0·79	$(1b_{3g})^{-1}$	$1b_{3u} \leftarrow 1b_{3g}$
^2A_g	14·7	0·81	$(3a_g)^{-1}$	$1b_{3u} \leftarrow 3a_g$
$^2B_{2u}$	15·9	0·71	$(1b_{2u})^{-1}$	$1b_{3u} \leftarrow 1b_{2u}$
$^2B_{2g}$	17·2	0·02	$(1b_{3u})^{-2} (2b_{2g})^1$	$2b_{2g} \leftarrow 1b_{3u}$
$^2B_{2u}$	18·2	0·02	$(1b_{3g})^{-1} (1b_{3u})^{-1} (1b_{2g})^1$	$1b_{2g} \leftarrow 1b_{3g}$
$^2B_{1u}$	19·2	0·61	$(2b_{1u})^{-1}$	$1b_{3u} \leftarrow 2b_{1u}$
$^2B_{1u}$	20·3	0·06	$(3a_g)^{-1} (1b_{3u})^{-1} (1b_{2g})^1$	$1b_{2g} \leftarrow 3a_g$
$^2B_{3g}$	21·9	0·00	$(1b_{2u})^{-1} (1b_{3u})^{-1} (1b_{2g})^1$	$1b_{2g} \leftarrow 1b_{2u}$
$^2B_{2u}$	22·1	0·06	$(1b_{3g})^{-1} (1b_{3u})^{-1} (1b_{2g})^1$	$1b_{2g} \leftarrow 1b_{3g}$
^2A_g	22·1	0·00	$(1b_{3u})^{-2} (4a_g)^1$	$4a_g \leftarrow 1b_{3u}$
$^2B_{2u}$	22·7	0·00	$(1b_{3u})^{-2} (2b_{2u})^1$	$2b_{2u} \leftarrow 1b_{3u}$
^2A_g	23·4	0·19	$(1b_{3u})^{-2} (5a_g)^1$	$5a_g \leftarrow 1b_{3u}$
$^2B_{1u}$	23·4	0·00	$(1b_{3u})^{-2} (3b_{1u})^1$	$3b_{1u} \leftarrow 1b_{3u}$
$^2B_{3u}$	23·9	0·00	$(1b_{3u})^{-2} (2b_{3u})^1$	$2b_{3u} \leftarrow 1b_{3u}$
$^2B_{3g}$	24·2	0·01	$(1b_{2u})^{-1} (1b_{3u})^{-1} (1b_{2g})^1$	$1b_{2g} \leftarrow 1b_{2u}$
$^2B_{1u}$	24·3	0·08	$(3a_g)^{-1} (1b_{3u})^{-1} (1b_{2g})^1$	$1b_{2g} \leftarrow 3a_g$
$^2B_{3u}$	24·5	0·00	$(1b_{2u})^{-1} (1b_{3g})^{-1} (1b_{2g})^1$	$1b_{2g}, 1b_{3u} \leftarrow 1b_{2u}, 1b_{3g}$
^2A_g	24·6	0·28	$(2a_g)^{-1}$	$1b_{3u} \leftarrow 2a_g$
^2A_g	25·1	0·02	$(1b_{3u})^{-2} (6a_g)^1$	$6a_g \leftarrow 1b_{3u}$
$^2B_{2u}$	25·2	0·00	$(1b_{3u})^{-2} (3b_{2u})^1$	$3b_{2u} \leftarrow 1b_{3u}$
$^2B_{3u}$	25·5	0·00	$(1b_{3u})^{-1} (3a_g)^{-1} (4a_g)^1$	$4a_g \leftarrow 3a_g$
$^2B_{3g}$	25·5	0·00	$(1b_{3u})^{-1} (1b_{3g})^{-1} (2b_{3u})^1$	$2b_{3u} \leftarrow 1b_{3u}$
$^2B_{3g}$	25·5	0·00	$(1b_{3u})^{-2} (2b_{3g})^1$	$2b_{3g} \leftarrow 1b_{3u}$
$^2B_{2g}$	25·7	0·00	$(1b_{3u})^{-2} (1b_{2g})^1$	$1b_{2g} \leftarrow 1b_{3u}$
$2B_{3g}$	25·9	0·00	$(1b_{3u})^{-1} (1b_{3g})^{-1} (2b_{3u})^1$	$2b_{3u} \leftarrow 1b_{3g}$
^2A_g	27·1	0·02	$(1b_{3u})^{-1} (2b_{1u})^{-1} (1b_{2g})^1$	$1b_{2g} \leftarrow 2b_{1u}$
^2A_g	27·6	0·01	$(1b_{3u})^{-2} (7a_g)^1$	$7a_g \leftarrow 1b_{3u}$
^2A_g	27·8	0·03	$(1b_{3u})^{-1} (3a_g)^{-1} (2b_{3u})^1$	$2b_{3u} \leftarrow 3a_g$
^2A_g	28·6	0·09	$(1b_{3u})^{-1} (2b_{1u})^{-1} (1b_{2g})^1$	$1b_{2g} \leftarrow 2b_{1u}$
^2A_g	28·6	0·01	$(3a_g)^{-1} (1b_{3u})^{-1} (2b_{3u})^1$	$2b_{3u} \leftarrow 3a_g$
^2A_g	28·9	0·04	$(1b_{3g})^{-2} (5a_g)^1$	$5a_g, 1b_{3u} \leftarrow (1b_{3g})^2$
^2A_g	29·1	0·02	$(1b_{3u})^{-2} (9a_g)^1$	$9a_g \leftarrow 1b_{3u}$
^2A_g	29·9	0·01	$(1b_{2u})^{-1} (1b_{3u})^{-1} (1b_{1g})^1$	$1b_{1g} \leftarrow 1b_{2u}$

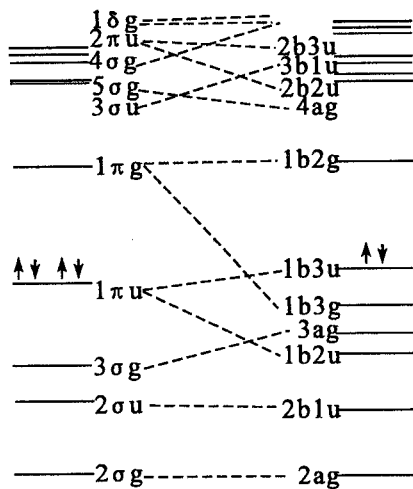[*]Only $S = \frac{1}{2}$ states are included. Beyond 26 eV, only states with large S^2 are included.

Fig. 1. Relative orbital energies of $C_2H_2^+$ (on left) and $C_2H_4^+$ (on right). The highest occupied orbitals are marked with arrows indicating the electron population in the neutral molecule. The virtual orbitals are those appearing in the first few excited states of the ion.
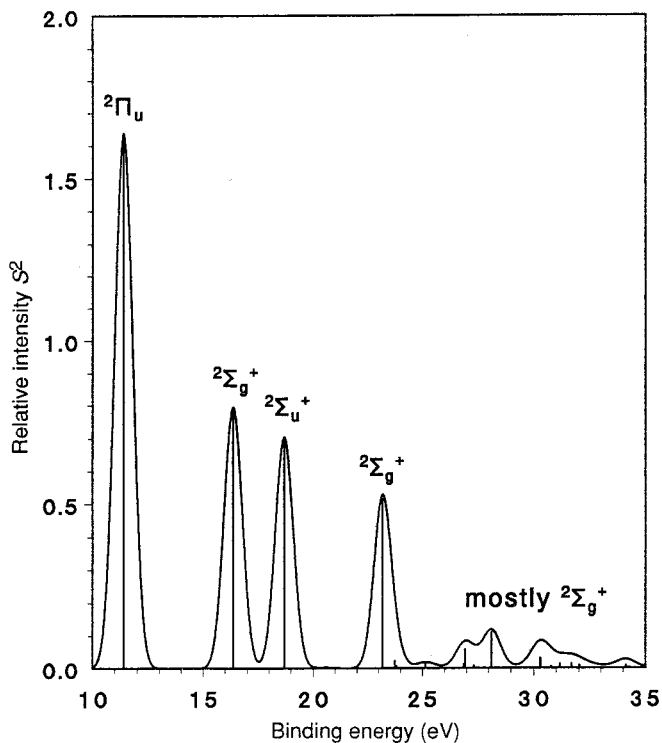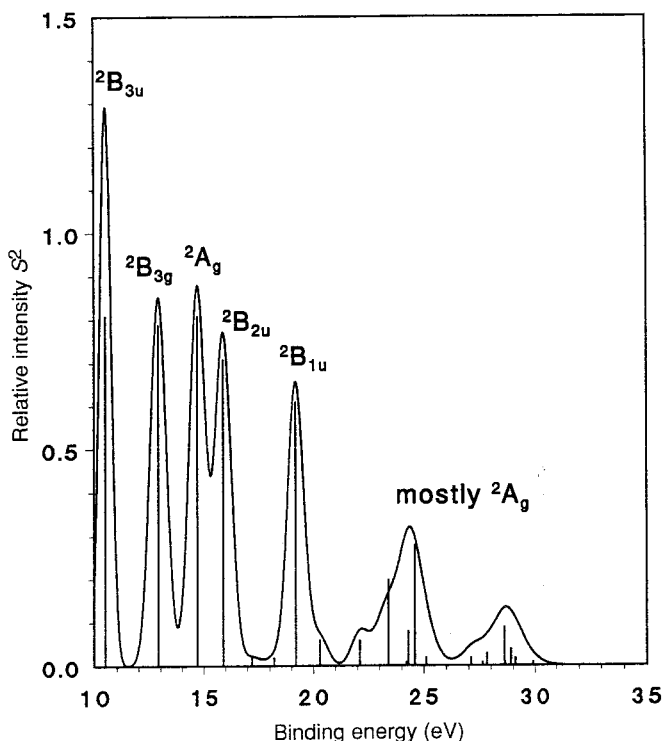

Fig. 2. A mock spectrum showing the calculated energy of the excited states of the $C_2H_2^+$ ion relative to C_2H_2 and the pole strength with peak widths from typical PES experiments.

The final result of the configuration selection in the calculations discussed here was a list of about 300,000 configurations for each symmetry from which up to 40 eigenvalues were extracted. The excitation energies for these states were correct to within $0 \cdot 3$ eV. The general distribution of pole strengths is reasonable except where very small pole strengths are involved. There also are a few cases where near degeneracy between a $1h$ configuration and a $2h$–$1p$ configuration causes a problem. When the connecting matrix element is small, the extent of mixing is extremely sensitive to the difference in energy between the configurations. This difference depends critically on the accuracy to which each state is described, so small changes in the basis set, MO construction, or configuration selection, have a large effect on the extent of mixing in the case of accidental near degeneracy.

Fig. 3. A mock spectrum showing the calculated energy of the excited states of $C_2H_4^+$ relative to C_2H_4 and the pole strength with peak widths from typical PES experiments.

3. Results for Acetylene and Ethylene

Tables 1 and 2 list a few of the states of the radical cation of acetylene, $HC \equiv CH^+$, and ethylene, $H_2C = CH_2^+$, in the energy range of interest. Missing from these tables are higher spin states and the $^2\Sigma^-$ states of acetylene. Also, the tables have been truncated in the higher energy region and only states with the largest pole strengths are shown. These states have been labeled by their dominant configuration rather than the minor primary hole component that

normally gives the PES intensity. With few exceptions, these states are single excitations from the ion ground state. Where the same configuration appears twice in the ethylene list, it is because there are two ways to form $S = \frac{1}{2}$ with three singly occupied orbitals. In the acetylene list, the same configuration may appear even more often, reflecting the various possible couplings of L_z. These tables can be compared with the sketch of orbital energies in Fig. 1. This allows a quick check to see that all the low energy transitions are accounted for. Clearly, no additional states are expected in the low energy range.
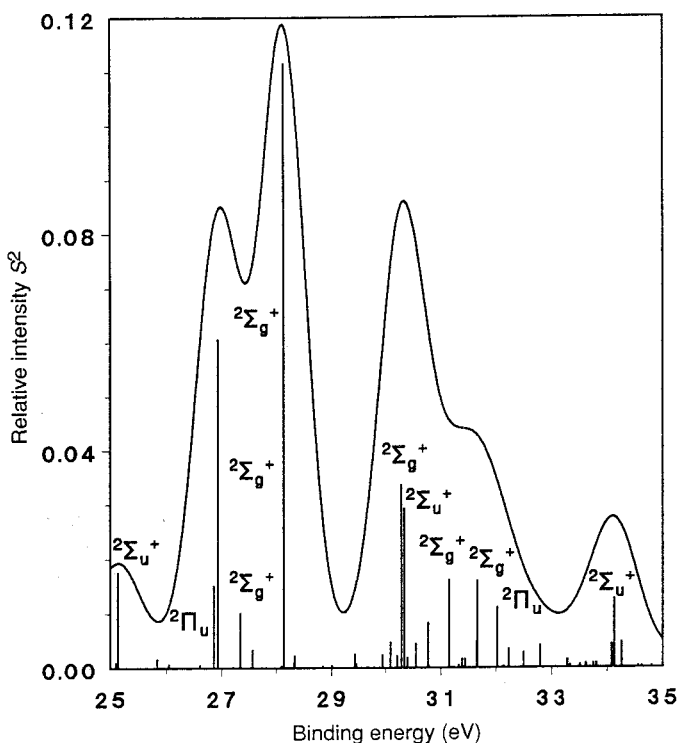
Fig. 4. An enlarged view of the satellite region of Fig. 2 for $C_2H_2^+$.

Figs 2 and 3 show a model of the PES spectrum reconstructed from these states. The area assigned to each peak has been chosen proportional to S^2 and the width was taken from the experimental spectrum. No actual accounting for variations in the transition moments has been done. Nevertheless, the picture recovers the essential features of the spectrum and allows a visualisation of the results in Tables 1 and 2. It is clear that most of the states of the ion are invisible in PES or EMS spectroscopy. Many of these would be easily seen in conventional optical spectra of the radical cations if light sources in the 0–20 eV range were available and a beam of the cations could be formed with sufficient number density.

The lowest four peaks in the acetylene spectra, Fig. 2, correspond to the four distinct energies of the filled valence orbitals. The region from 25–35 eV has considerable intensity with several overlapping peaks in the experimental PES
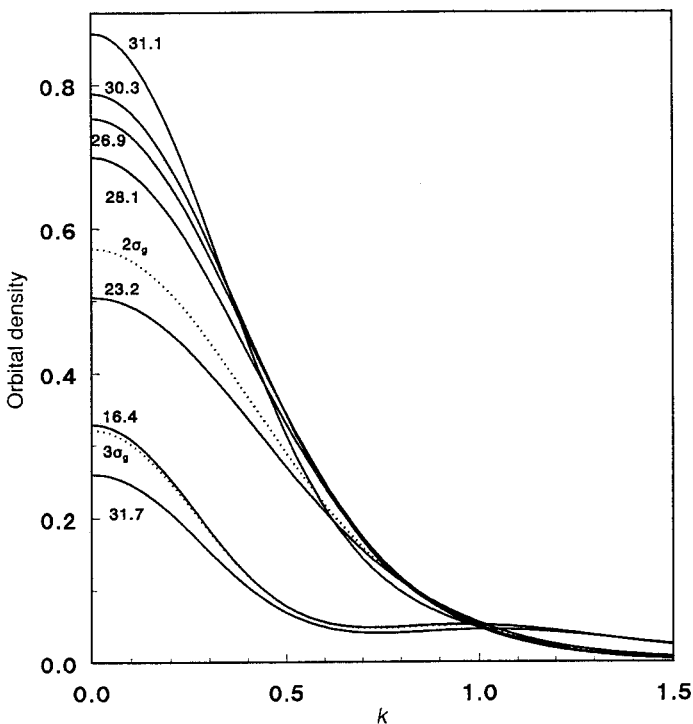
Fig. 5. The spherically averaged square of the Dyson orbital in momentum space plotted against the momentum (in atomic units) for $C_2H_2^+$. The neutral molecule Hartree–Fock orbitals are shown as dotted curves. Each curve is labeled by the energy of the $^2\Sigma_g{}^+$ state from which it was derived (see Table 1 and Fig. 4).

spectra and various assignments have been suggested (Cederbaum *et al.* 1986; Dixon *et al.* 1977; Cavell and Allison 1978; Cederbaum *et al.* 1978; Bradshaw *et al.* 1980; Machado *et al.* 1982; Müller *et al.* 1982; Svensson *et al.* 1984, 1988; Wasada and Hirao 1989; Weigold *et al.* 1991; Koch *et al.* 1991). Fig. 4 shows an enlarged view of this region with the states we have predicted. Clearly most of the intensity is from $^2\Sigma_g^+$ states. Examination of the Dyson orbitals for these peaks up to 30·5 eV show that they resemble the $2\sigma_g$ orbital. There also is appreciable intensity from $^2\Sigma_u^+$ (with a Dyson orbital resembling $2\sigma_u$) and from $^2\Pi_u$ (with a Dyson orbital resembling $1\pi_u$). Beyond 30·5 eV, the $^2\Sigma_g^+$ states also have appreciable contributions from the $3\sigma_g$ orbital. This can be seen in Fig. 5 which shows the spherically averaged momentum distribution for the normalised Dyson orbitals from the states with the largest pole strengths. The state at 31·1 eV has a normalised Dyson orbital that is approximately $0·8(2\sigma_g)+0·6(3\sigma_g)$, while the Dyson orbital for the 31·7 eV state is nearly pure $3\sigma_g$. Thus, the region from 26–31 eV is mostly a satellite to the $2\sigma_g^{-1}$ primary hole while the region from 31 to 32 eV is mostly a $3\sigma_g^{-1}$ satellite. Our $(1\pi_u)^{-2}$ $(^1\delta_g)^1$ $^2\Sigma_g^+$ state at 28·1 eV seems to have been missed in previous calculations that use less extensive basis sets with fewer functions of δ_g symmetry.

The ethylene spectrum is even more complicated because the $2p$–$1h$ states complicate the primary hole $(2a_g)^{-1}$ region as well as the satellite region. As shown in Fig. 6 in an enlarged view, the $(2\sigma_g)^{-1}$ primary hole is split by near degeneracy with the $2h$–$1p$, $1b_{2g} \leftarrow 1b_{1u}$ excitation from the $1b_{3u}$ hole state. This same configuration with a different spin coupling appears in the satellite region with a number of other ^2A_g states, all borrowing intensity from the $(2a_g)^{-1}$ primary hole. The 'twinning' of the primary hole peak was first predicted by Cederbaum *et al.* (1978). The assignment of the satellite to ^2A_g was first done by Martin and Davidson (1977a, b) and was verified by EMS measurements (Coplan *et al.* 1978; Dixon *et al.* 1978). Other workers have assigned the satellite intensity to $^2B_{1u}$ (Wasada and Hirao 1989; Gelius 1974; Carlier and Botter 1979; Banna and Shirley 1976; Nakatsuji 1984).
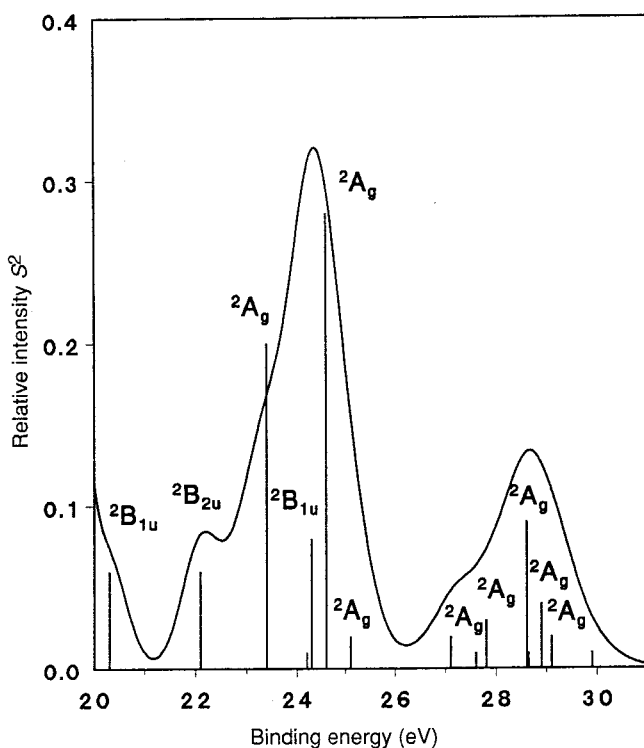

Fig. 6.   An enlarged view of the satellite and $2a_g$ region of Fig. 3 for $C_2H_4^+$.

The extent to which these ^2A_g peaks all give the same Dyson orbital can be examined in detail. Fig. 7 shows the square of the normalised, spherically-averaged Dyson orbitals in momentum space for five of the ^2A_g states. These five states most nearly correspond to the $3a_g^{-1}$ primary hole, the split $(2a_g)^{-1}$ primary hole, and the two dominant states in the satellite region. For comparison, the canonical Hartree–Fock orbitals of the neutral ground state are also shown. The usual approximation that the normalised Dyson orbitals are nearly the same as the Hartree–Fock orbitals applies well for the primary holes. The Dyson orbital

for the satellite is similar to the $2a_g$ orbital, but is about 30% larger at low momentum. Examination of the expansion of the Dyson orbital for the satellite shows it is approximately 90% $2\sigma_g$ and 10% $3\sigma_g$ because of small contributions from the $(3\sigma_g)^{-1}$ configuration to the satellite peak wave function.
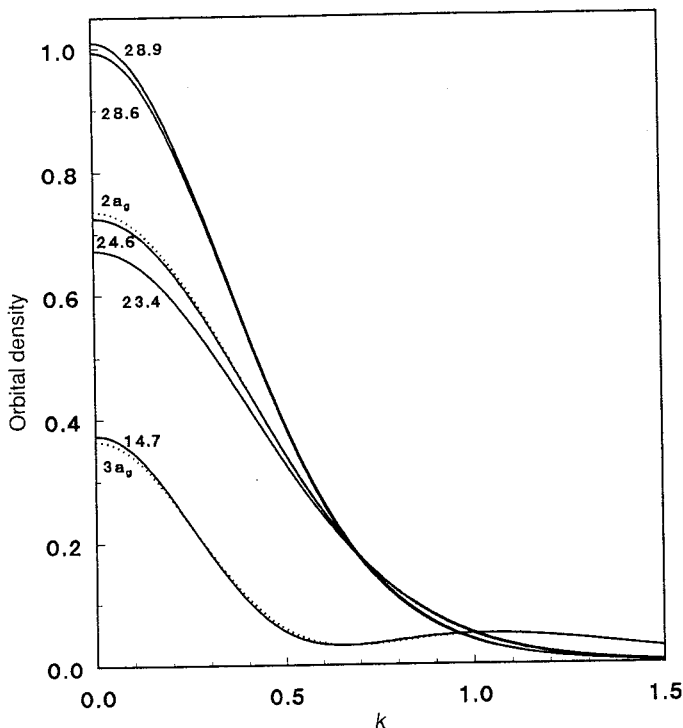

Fig. 7. The spherically averaged square of the Dyson orbital in momentum space plotted against the momentum (in atomic units) for $C_2H_4^+$. The neutral molecule Hartree–Fock orbitals are shown as dotted curves. Each curve is labeled by the energy of the ^2A_g state from which it was derived (see Table 2 and Fig. 6).

4. Conclusions

These calculations have shown that the satellite region for acetylene contains contributions from states of $^2\Sigma_g^+$, $^2\Sigma_u^+$ and $^2\Pi_u$ symmetry. The calculations have also shown that the Dyson orbitals for satellites cannot be assumed to be identical with those for primary holes.

Acknowledgment

References

Åberg, T. (1967). *Phys. Rev.* **156**, 35.
Banna, M. S., and Shirley, D. A. (1976). *J. Elect. Spectrosc. Relat. Phenom.* **8**, 255.
Bawagan, A. O., Brion, C. E., Davidson, E. R., and Feller, D. (1987). *Chem. Phys.* **113**, 19.

Bawagan, A. O., Brion, C. E., Davidson, E. R., Boyle, C. M., and Frey, R. F. (1988a). *Chem. Phys.* **128**, 439.

Bawagan, A. O., Müller-Fiedler, R., Brion, C. E., Davidson, E. R., and Boyle, C. M. (1988b). *Chem. Phys.* **120**, 335.

Bradshaw, A. M., Eberhardt, W., Levinson, H. J., Domcke, W., and Cederbaum, L. S. (1980). *Chem. Phys. Lett.* **70**, 36.

Carlier, J., and Botter, R. (1979). *J. Elect. Spectrosc. Relat. Phenom.* **17**, 91.

Cavell, R. G., and Allison, D. A. (1978). *J. Chem. Phys.* **69**, 159.

Cederbaum, L. S., Domcke, W., Schirmer, J., von Niessen, W., Diercksen, G. H. F., and Kraemer, W. P. (1978). *J. Chem. Phys.* **69**, 1591.

Cederbaum, L. S., Domcke, W., Shirmer, J., and von Niessen, W. (1986). *Adv. Chem. Phys.* **65**, 115.

Clark, S. A. C., Brion, C. E., Davidson, E. R., and Boyle, C. (1989a). *Chem. Phys.* **136**, 55.

Clark, S. A. C., Weigold, E., Brion, C. E., Davidson, E. R., Frey, R. F., Boyle, C. M., von Niessen, W., and Schirmer, J. (1989b). *Chem. Phys.* **134**, 229.

Clark, S. A. C., Reddish, T. J., Brion, C. E., Davidson, E. R., and Frey, R. F. (1990). *Chem. Phys.* **143**, 1.

Coplan, M. A., Migdall, A. L., Moore, J. H., and Tossell, J. A. (1978). *J. Am. Chem. Soc.* **100**, 5008.

Davidson, E. R., Feller, D., Boyle, C. M., Adamowicz, L., Clark, S. A. C., and Brion, C. E. (1990). *Chem. Phys.* **147**, 45.

Desjardins, S. J., Bawagan, A. D. O., Tan, K. H., Wang, Y., and Davidson, E. R. (1994). *Chem. Phys. Lett.* **227**, 519.

Desjardins, S. J., Bawagan, A. D. O., Liu, Z. F., Tan, K. H., Wang, Y., and Davidson, E. R. (1995). *J. Chem. Phys.*, **102**, 6385.

Dixon, A. J., McCarthy, I. E., Weigold, E., and Williams, G. R. J. (1977). *J. Elect. Spectrosc. Relat. Phenom.* **12**, 239.

Dixon, A. J., Hood, S. T., Weigold, E., and Williams, G. R. J. (1978). *J. Elect. Spectrosc. Relat. Phenom.* **14**, 267.

Duffy, P., Casida, M. E., Brion, C. E., and Chong, D. P. (1992a). *Chem. Phys.* **159**, 347.

Duffy, P., Clark, S. A. C., Brion, C. E., Casida, M. E., Chong, D. P., Davidson, E. R., and Maxwell, C. (1992b). *Chem. Phys.* **165**, 183.

Feller, D., and Davidson, E. R. (1981). *J. Chem. Phys.* **74**, 3977.

French, C. L., Brion, C. E., Bawagan, A. O., Bagus, P. S., and Davidson, E. R. (1988a). *Chem. Phys.* **121**, 315.

French, C. L., Brion, C. E., and Davidson, E. R. (1988b). *Chem. Phys.* **122**, 247.

Gelius, U. (1974). *J. Elect. Spectrosc. Relat. Phenom.* **5**, 985.

Hollebone, B. P., Brion, C. E., Davidson, E. R., and Boyle, C. (1993a). *Chem. Phys.* **173**, 193.

Hollebone, B. P., Duffy, P., Brion, C. E., Wang, Y., and Davidson, E. R. (1993b). *Chem. Phys.* **178**, 25.

Hollebone, B. P., Zheng, Y., Brion, C. E., Davidson, E. R., and Feller, D. (1993c). *Chem. Phys.* **171**, 303.

Hollebone, B. P., Neville, J. J., Zheng, Y., Brion, C. E., Wang, Y., and Davidson, E. R. (1995). *Chem. Phys.* **196**, 13.

Koch, A., Schmidbauer, M., Feldhaus, J., Randall, K. J., and Bradshaw, A. M. (1991). *J. Elect. Spectrosc. Relat. Phenom.* **51**, 527.

McCarthy, I. E., and Weigold, E. (1976). *Phys. Rev. C* **27**, 275.

Machado, L. E., Leal, E. P., Csanak, G., McKoy, B. V., and Langhoff, P. W. (1982). *J. Elect. Spectrosc. Relat. Phenom.* **25**, 1.

Manne, R., and Åberg, T. (1970). *Chem. Phys. Lett.* **7**, 282.

Martin, R. L., and Davidson, E. R. (1977a). *Chem. Phys. Lett.* **51**, 237.

Martin, R. L., and Davidson, E. R. (1977b). *Phys. Rev. A* **16**, 1341.

Martin, R. L., Davidson, E. R., Banna, M. S., Wallbank, B., Frost, D. C., and McDowell, C. A. (1978). *J. Chem. Phys.* **68**, 5006.

Martin, R. L., Daasch, W. R., and Davidson, E. R. (1979). *J. Chem. Phys.* **71**, 2375.

Maxwell, C. J., Machado, F. B. C., and Davidson, E. R. (1992). *J. Am. Chem. Soc.* **114**, 6496.

Moghaddam, M. S., Dejardins, S.J., Bawagan, A. D. O., Tan, K. H., Wang, Y., and Davidson, E. R. (1995). *J. Chem. Phys.*, in press.

Müller, J., Arneberg, R., Ågren, H., Manne, R., Malmqvist, P.-Å., Svensson, S., and Gelius, U. (1982). *J. Chem. Phys.* **77**, 4895.

Murray, C., and Davidson, E. R. (1992). *Chem. Phys. Lett.* **190**, 231.

Nakatsuji, H. (1984). *J. Chem. Phys.* **80**, 3703.

Rehr, J. J., Stern, E. A., Martin, R. L., and Davidson, E. R. (1978). *Phys. Rev.* B **17**, 560.

Rossi, A. R., and Davidson, E. R. (1992). *J. Phys. Chem.* **96**, 10682.

Stöhr, J., Jaeger, R., and Rehr, J. J. (1983). *Phys. Rev. Lett.* **51**, 821.

Svensson, S., Malmqvist, P.-Å., Adam, M. Y., Lablanquie, P., Morin, P., and Nenner, I. (1984). *Chem. Phys. Lett.* **111**, 574.

Svensson, S., Zdansky, E., Gelius, U., and Ågren, A. (1988). *Phys. Rev.* **37**, 4730.

Thomas, T. D. (1984). *Phys. Rev. Lett.* **52**, 417.

Wasada, H., and Hirao, K. (1989). *Chem. Phys.* **138**, 277.

Weigold, E., Zhao, K., and von Niessen, W. (1991). *J. Chem. Phys.* **94**, 3468.